Continuous-wave coherent imaging with terahertz quantum cascade lasers using electro-optic harmonic sampling

M. Ravaro, V. Jagtap, G. Santarelli, C. Sirtori, L. H. Li et al.

Additional information on Appl. Phys. Lett.

Continuous-wave coherent imaging with terahertz quantum cascade lasers using electro-optic harmonic sampling

M. Ravaro,[1,a)] V. Jagtap,[1] G. Santarelli,[2] C. Sirtori,[1] L. H. Li,[3] S. P. Khanna,[3,b)] E. H. Linfield,[3] and S. Barbieri[1,c)]

[1]*Laboratoire Matériaux et Phénomènes Quantiques (MPQ) and CNRS, UMR 7162,*
Université Paris-Diderot, 10, rue A. Domont et L. Duquet, 75205 Paris, France
[2]*Laboratoire Photonique, Numérique et Nanosciences (LP2N) and CNRS, UMR 5298,*
Université de Bordeaux 1, Institut d'Optique, 351 cours de la Libération, 33405 Talence, France
[3]*School of Electronic and Electrical Engineering, University of Leeds, Leeds LS2 9JT, United Kingdom*

We demonstrate a coherent imaging system based on a terahertz (THz) frequency quantum cascade laser (QCL) phase-locked to a near-infrared fs-laser comb. The phase locking enables coherent electro-optic sampling of the continuous-wave radiation emitted by the QCL through the generation of a heterodyne beat-note signal. We use this beat-note signal to demonstrate raster scan coherent imaging using a QCL emitting at 2.5 THz. At this frequency the detection noise floor of our system is of 3 pW/Hz and the long-term phase stability is <3°/h, limited by the mechanical stability of the apparatus. © 2013 American Institute of Physics. [http://dx.doi.org/10.1063/1.4793424]

Significant scientific effort over recent years has aimed at the realization of terahertz (THz) frequency imaging systems based on quantum cascade lasers (QCLs). Even though the continuous-wave output power of these devices can be as high as tens of mW,[1–3] there are still several technological issues that need to be addressed with the detection in order to realize a system that is sufficiently sensitive, as well as fast and compact. For this reason several groups have tested different detection techniques and configurations. Incoherent imaging systems have been demonstrated using Golay cells, pyroelectric detectors, cryogenically cooled bolometers, and commercial focal plane array microbolometric cameras.[4–7] More recently, a QCL-based imaging system was also demonstrated using an amorphous-silicon microbolometric camera that was specifically developed for operation in the THz range.[8] Coherent imaging techniques have also been reported in the literature, including a pseudo-heterodyne technique based on the mixing between the longitudinal modes of a multimode QCL,[9] self-mixing,[10] and exploiting the heterodyne mixing between a QCL and gas laser.[11] In the latter, the THz QCL was frequency-locked to the gas laser line in order to reduce the phase instability of the emitted radiation field and allow the application of an inverse synthetic aperture radar technique. Our work here is based on a coherent imaging technique that was first demonstrated by Loffler et al.,[12] who used a harmonic of the repetition rate of a mode-locked Ti:Sa laser as a local oscillator and mixed it with a quartz-stabilized Gunn oscillator emitting at 0.6 THz. In that case, both sources were free running since their intrinsic phase/frequency stability was sufficiently high. However, recently, it has been demonstrated that although THz QCLs have sub kHz quantum noise limited linewidths,[13,14] up to a

Fourier frequency of ~10 kHz they are affected by a ~ $1/f^2$ noise component, giving rise to the line broadening and frequency drifts that have been observed in several heterodyne experiments.[15,16] As a consequence the scheme of Ref. 12 cannot be implemented with a THz QCL without active stabilization.

Over the last few years, techniques have been developed to stabilize THz QCLs to near-IR frequency combs produced by fs-mode-locked fiber lasers.[17–20] These exploit the sampling (electro-optic or photoconductive) of the radiation field emitted by the QCL using the mode-locked pulses from the fs-laser. In the RF domain, this sampling gives rise to a series of heterodyne beat signals between the harmonics of the fs-laser repetition rate and the THz field. The lowest frequency beat-note signal can be fed into standard RF electronics and used to phase-lock the QCL to the fs-laser repetition rate thus eliminating the phase jitter between the two sources. The sub-Hz beat-note linewidth obtained with this technique allows the coherent accumulation of the signal from the QCL over long integration times and the achievement of high signal-to-noise ratios.[20] In the work presented here, this harmonic sampling technique has been used to implement a coherent imaging setup using a single-mode 2.5 THz QCL and a frequency doubled fs-laser comb as local oscillator. We have achieved imaging with a noise detection limit of 3 pW/Hz and a long-term phase stability of less than 3°/h. The maximum detection bandwidth is determined only by the sampling rate and not by the detector rise time as found when using a Golay cell or bolometer.

The QCL used in our experiments operates at 2.5 THz and is based on a 2.5 mm-long, 240 µm-wide, ridge-waveguide Fabry-Perot cavity that was fabricated by optical-lithography and wet-etching (details on the waveguide and active region design can be found in Ref. 3). The QCL was kept at a stabilized temperature of 20 K using a continuous-flow, liquid-helium cryostat, and driven at a constant current of 1.49 A with a commercial power supply. Under these operating conditions, the emission is single-mode and the

---

output power measured with a calibrated THz power-meter (Thomas Keating Ltd.) is $\approx 2\,mW$. For the near-IR laser comb, we used a frequency doubled, mode-locked fs-fiber laser (Menlo Systems, M-fiber) operating at $\lambda = 780\,nm$ and emitting a train of $\sim 100\,fs$-long pulses at a repetition rate of $\sim 250\,MHz$.

The experimental apparatus is shown in Fig. 1 and is based on two identical electro-optic (EO) detection units, labeled EO1 and EO2, that are used, respectively, to (i) lock the QCL frequency to the fs-laser comb and (ii) detect the QCL beam after it has been reflected by the imaged target.[12] For our experiments, the QCL and near-IR comb beams are each split into two using separate beam splitters (labeled BS), and detection is achieved in both units by collinearly focusing the beams onto a 2 mm-thick, $\langle 1, \bar{1}, 0 \rangle$ oriented ZnTe crystal, which is followed by $\lambda/4$ and $\lambda/2$ waveplates and a polarizing beam splitter. These elements form an ultrafast, near-IR electro-optic amplitude modulator driven by the THz ac field (see Ref. 17 for details of the operating principle). Assuming for simplicity that the QCL is single mode, this modulator generates two sideband combs at $\pm 2.5\,THz$ from the comb carrier centered at 780 nm (385 THz). Since the comb bandwidth is approximately twice the QCL frequency, the carrier overlaps

with the sideband combs producing a series of heterodyne beat-notes oscillating at frequencies $|(\nu_{QCL} - n \times f_{rep})|$, where ν_{QCL} is the emission frequency of the QCL, f_{rep} is the fs-laser repetition rate (250 MHz), and n is an integer number.[17] Therefore, the lowest frequency beating, f_{beat}, corresponds to $n = Int(\nu_{QCL}/f_{rep}) \sim 10^4$ (=2.5 THz/250 MHz) and has a frequency $f_{beat} < f_{rep}/2 \sim 125\,MHz$. This beat-note is detected using a shot-noise limited balanced detection, based on a pair of Si-photodiodes, and followed by a fast amplifier with a bandwidth of approximately 200 MHz. Ultimately, the detection bandwidth of the system is limited by the Nyquist criterion to half the sampling rate, i.e., 125 MHz.

To lock the QCL frequency, the beat-note generated by EO1 is compared, using a mixer, to a signal at $f_{RF1} \sim 10\,MHz$ produced by an RF synthesizer (RF1). The error signal oscillating at $(f_{beat} - f_{RF1})$ is then used to control the QCL current through a purpose designed phase-lock loop (PLL) circuit with a bandpass of $\sim 2\,MHz$, and phase-lock ν_{QCL} to the $\sim 10^4$ harmonic of the fs-laser repetition rate. In the inset of Fig. 2 we show an example of the spectrum of the phase-locked f_{beat} beat signal, acquired with a spectrum analyzer with a resolution bandwidth of 10 Hz and a THz power impinging on EO1 of 250 μW. This phase-locking is critical to allow image acquisition using a conventional lock-in amplifier (see below).

The second half of the QCL beam is focused on the imaged target using an f/1, gold-coated, off-axis parabolic mirror (identical to the one used to collimate the QCL beam). Approximately half of the THz radiation reflected from the target is finally focused on EO2. As found in previous experiments,[13,17–19] the QCL is affected by optical feedback which, in this case, mainly arises from the fraction of the beam reflected from the target that is transmitted through the beam splitter. As shown in Ref. 13, optical feedback has a strong influence on the QCL frequency noise. In particular, in the present case, the phase of the radiation reflected into the QCL cavity, as well as the intensity, changed markedly when the beam was raster scanned across the imaged object
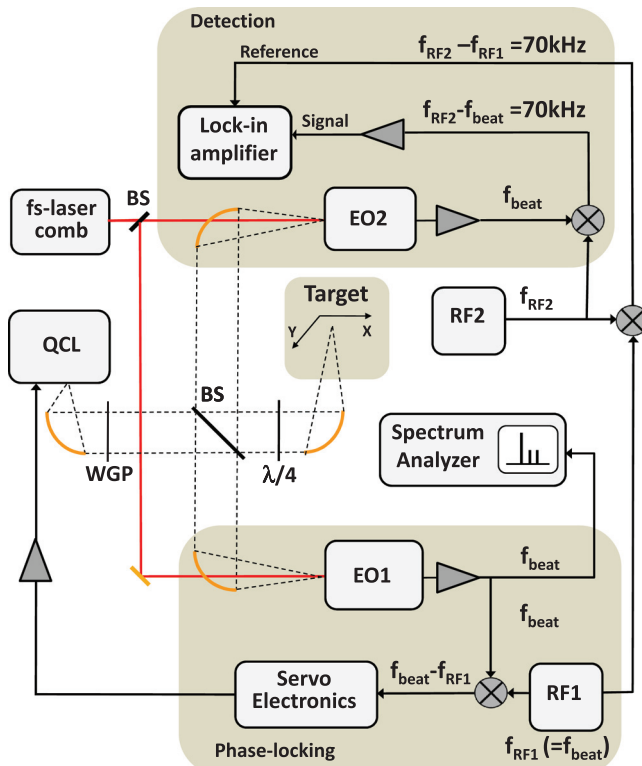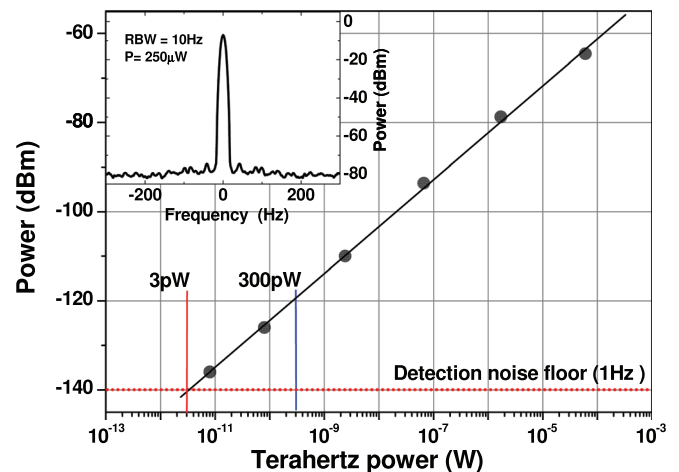

FIG. 1. Experimental apparatus. The fs-laser comb and QCL beams are split into two parts, using two beam splitters (BS), and are focused onto EO detection units EO1 and EO2. EO1 is used to phase-lock f_{beat} to f_{RF1}, and therefore to phase-lock ν_{QCL} to $\sim 10^4 \times f_{rep}$. EO2 is used to detect the THz radiation back-reflected from the imaged target. This is achieved by mixing f_{beat} (=f_{RF1}) with $f_{RF2} = f_{beat} + 70\,kHz$ and by monitoring the difference frequency, oscillating at 70 kHz, with a lock-in amplifier. The reference of the lock-in is obtained from the difference frequency $f_{RF2} - f_{RF1} = 70\,kHz$. All mirrors used to collimate and focus the radiation from the QCL are 90° off-axis, gold coated parabolic mirrors. The fs-laser comb is a frequency doubled 1550 nm fiber laser emitting a train of $\sim 100\,fs$ pulses at a repetition rate $f_{rep} = 250\,MHz$. There is approximately 15 mW of optical power at 780 nm impinging on each EO detection unit.

FIG. 2. Measurement of the noise equivalent power of the imaging system. The THz power focused on EO2 was decreased from 60 μW to 8 pW using calibrated attenuators. The noise floor at $-140\,dBm$ is set by the shot noise of EO2 in a 1 Hz bandwidth and gives a noise equivalent power of 3 pW/Hz. Inset: spectrum of f_{beat} detected on EO1 and recorded on the spectrum analyzer with a resolution bandwidth of 10 Hz. The THz power used for EO detection is 250 μW.

owing to changes in the surface profile and morphology. We found experimentally that this effect could suddenly drive the QCL out of lock, thus compromising the image acquisition. To limit the effect of this feedback we inserted an optical isolator, consisting of a wire-grid polarizer (WGP) oriented parallel to the TM-polarised light from the QCL. This was followed, after the beam splitter, by a 3.1 mm-thick, quartz quarter-wave plate with its fast-axis at 45° with respect to the polarizer.[13] As a result, after the quarter-wave plate, the THz light emitted by the QCL is left circularly polarised, and the polarisation is changed from left- to right-circular after reflection from the target. Going back through the quarter-wave plate the reflected beam recovers its linear polarisation, now orthogonal to the wire grid polariser (and to the QCL polarisation), thus providing the isolation. Using a power meter we measured an isolation of $\sim$16 dB. However, this was not sufficient to completely suppress the random un-locking of f_{beat} during image acquisition. Therefore an additional $\sim$10 dB of attenuation was added ($\sim$5 dB attenuation per pass).

For the measurement of the radiation reflected by the imaged object, we used a standard lock-in amplifier (SRS, model SR830) and a reference oscillator, RF1. As shown in Fig. 1, in order to bring $f_{RF1} = 10$ MHz ($= f_{beat}$) within the lock-in reference frequency range (1 mHz–100 kHz), the latter was down-converted to 70 kHz by mixing with another synthesiser, labelled RF2, oscillating at $f_{RF2} = 10$ MHz $+ 70$ kHz. The same synthesiser was mixed with f_{beat} generated by EO2 to provide the lock-in input signal. It is important to note that the phase-locking of ν_{QCL} is a crucial requirement for the realization of our coherent imaging system. Indeed, whilst in principle the free-running f_{beat} generated in EO1 could be used as a reference to demodulate the output of EO2, as in Ref. 12, in practice this is not possible. In fact, without phase-locking, the coherence between ν_{QCL} and f_{rep} is dominated by the low frequency noise component of ν_{QCL}, proportional to $\sim 1/f^2$, produced by mechanical vibrations and thermal and/or current fluctuations in the device.[13,14] As can be derived from the frequency noise spectral density of the QCL (identical to the present one) reported in Ref. 13, this generates an f_{beat} with an "instantaneous" linewidth of the order of 10 kHz on a 1 ms timescale, and subject to drifts of several MHz/s.[15,16,21] As a consequence the "free running" f_{beat} is not sufficiently stable to provide a reference signal for typical commercial DSP lock-in amplifiers including the one used here.[22] On the other hand, phase-locking of ν_{QCL} ensures the coherence with f_{rep}, eliminating their mutual jitter, and thus allows using f_{beat} (or RF1) as a reference.

Before proceeding to the image acquisition, we evaluated the sensitivity of our EO detection. Using a calibrated power meter, we measured THz powers of 250 μW and 60 μW impinging on the ZnTe crystals of EO1 and EO2, respectively. Given the 2 mW emitted power from the THz QCL, these values are in agreement with the attenuations from the optical elements shown in Fig. 1, including the attenuator used to decrease the optical feedback and, in the case of EO2, the reflection from the flat part of a 10 cent Euro coin that we used as a test target for our imaging system. In Fig. 2 we show the power in dBm of the phase-locked f_{beat} measured at the output of EO2 with a spectrum

analyzer with a resolution bandwidth of 1 Hz. The THz power was progressively attenuated from 60 μW to 10 pW by superimposing up to 14 A4 paper sheets. Down to 2 nW, the power was measured with a Golay cell detector that had been previously calibrated using a THz absolute power meter, while the two points below the 300 pW detection limit of the Golay cell were obtained using calibrated attenuators. The noise floor of -140 dBm is determined by the shot noise of the photocurrent generated by the 15 mW of near-IR power incident on the balanced detection and corresponds to the minimum detectable THz power of $\sim$3 pW (3 pW/Hz noise equivalent power). This is consistent with the spectrum of Fig. 2 (inset) at the output of EO1 where 250 μW of THz power yielded a SNR of $\sim$70 dB in a 10 Hz bandwidth, which corresponds to a noise equivalent power of $\sim$2.5 pW/Hz (the SNR scales linearly with the bandwidth).

Figs. 3(a)–3(c) show, respectively, the amplitude, power, and phase image in grey-colour scale of a 10 cent Euro coin, obtained by raster scanning the object in the focal plane of the mirror using a motorized XY stage. The image was obtained by continuous line scanning along the X direction (from left to right in the figure) at a speed of 2.2 mm/s, with a step between each line of 100 μm in the Y direction (the acquisition rate along the X direction was set to obtain the same spatial resolution of 100 μm). The lock-in time constant was 30 ms, which allowed a dynamic range of 60 dB, as shown in Fig. 3(b). The width of the vertical lines on the left
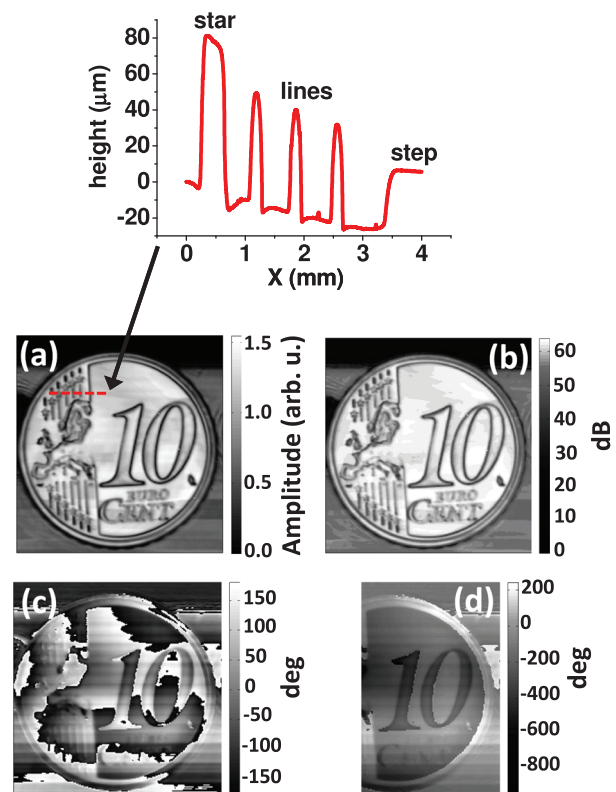

FIG. 3. THz image of a 10 cent Euro coin: (a) amplitude, (b) power, (c) raw phase image, and (d) phase image corrected for the limited phase range of the lock-in amplifier. The coin diameter is 19.75 mm. The image was acquired with lines scans from left to right at a speed of 2.2 mm/s, with a step between each line of 100 μm in the vertical direction. The lock-in amplifier time constant was set to 30 ms. Top: height profile obtained by scanning with a profilometer along the red dashed line of (a).

side of the coin was measured with a profilometer (top graph in Fig. 3) and was found to be 160 μm, showing that the system resolution is diffraction limited. This means an improvement of a factor $\sim$4, i.e. the wavelength scale factor, with respect to the resolution reported in Ref. 12. Fig. 3(c) displays the phase image, as recorded from the lock-in amplifier. As expected, compared to the amplitude or power plots where the edges of the reliefs appear very clear in black owing to scattering, here the various reliefs are displayed in different grey colors corresponding to different heights, and hence different phases owing to changes in the optical path. By monitoring the phase with time we observed a phase stability with fluctuations of $\pm 1^\circ$ on a s timescale, and a shift of $\leq 3^\circ$/h, corresponding to an uncertainty of $< 1\,\mu$m in the determination of the profile height. This phase stability is completely limited by the mechanical stability of the experimental apparatus. We verified with the profilometer that the height of most of the features is larger than $\lambda/2 = 60\mu$m; furthermore, the phase displayed by the lock-in amplifier is limited to $\pm\pi$, which reduces the effective length over which the phase changes continuously to $\lambda/4$. This, together with the fact that the coin is not perfectly parallel to the focal plane (a $\sim 0.3^\circ$ inclination is enough to produce a phase change of 2π across the coin), partially explains why the phase image does not display clearly the different shapes. Another difficulty is related to small details, such as the stars and stripes on the top left corner, where the size is close to the resolution limit of the system, resulting in a poor phase contrast. Moreover, as shown by the height profile in Fig. 3, some of the details such as the vertical lines have a height that is close to $\lambda/2$. In contrast, the amplitude image, resulting from scattering, allows much clearer identification of these details. Fig. 3(d) displays a partially processed phase image where the effect of the limited phase-range of the lock-in amplifier has been partially removed by adding or subtracting 2π to a fraction of the pixels of Fig. 3(c).

The imaging speed in these experiments is solely limited by the speed of the acquisition software. From Fig. 2, an integration time of 10 μs would still allow a signal to noise ratio of more than 30 dB, which would allow acquisition of Fig. 3 without degradation. This could be achieved by replacement of the XY translation stage with a fast steering mirror, enabling acquisition within a few seconds.

[1]S. Kumar, Q.Hu, and J. L. Reno, Appl. Phys. Lett. **94**, 131105 (2009).

[2]G. Xu, R. Colombelli, S. P. Khanna, A. Belarouci, X. Letartre, L. Li, E. H. Linfield, A. G. Davies, H. Beere, and D. A. Ritchie, Nat. Comm. **3**, 952 (2012).

[3]S. Barbieri, J. Alton, J. Fowler, H. E. Beere, E. H. Linfield, and D. A. Ritchie, Appl. Phys. Lett. **85**, 1674 (2004).

[4]K. L. Nguyen, M. L. Johns, L. F. Gladden, C. H. Worrall, P. Alexander, H. E. Beere, M. Pepper, D. A. Ritchie, J. Alton, S. Barbieri, and E. H. Linfield, Opt. Express **14**, 2123 (2006).

[5]P. Dean, M. U. Shaukat, S. P. Khanna, M. Lachab, A. Burnett, A. G. Davies, E. H. Linfield, and S. Chakraborty, Opt. Express **16**, 5997 (2008).

[6]J. Darmo, V. Tamosiunas, G. Fasching, J. Kröll, K. Unterrainer, M. Beck, M. Giovannini, J. Faist, C. Kremser, and P. Debbage, Opt. Express **12**, 1879 (2004).

[7]A. W. M. Lee, Q. Qin, S. Kumar, B. S. Williams, and Q. Hu, Appl. Phys. Lett. **89**, 141125 (2006).

[8]F. Simoens, J. Meilhan, B. Delplanque, S. Gidon, G. Lasfargues, J. L. Dera, D. T. Nguyen, J. L. Ouvrier-Buffet, S. Pocas, T. Maillou, O. Cathabard, and S. Barbieri, Proc. SPIE **8363**, 83630D (2012).

[9]S. Barbieri, J. Alton, C. Baker, T. Lo, H. E. Beere, and D. Ritchie, Opt. Express **13**, 6497 (2005).

[10]P. Dean, Y. L. Lim, A. Valavanis, R. Kliese, M. Nikolic, S. P. Khanna, M. Lachab, D. Indjin, Z. Ikonic, P. Harrison, A. D. Rakić, E. H. Linfield, and A. G. Davies, Opt. Lett. **36**, 2587 (2011).

[11]A. A. Danylov, T. M. Goyette, J. Waldman, M. J. Coulombe, A. J. Gatesman, R. H. Giles, X. Qian, N. Chandrayan, S. Vangala, K. Termkoa, W. D. Goodhue, and W. E. Nixon, Opt. Express **18**, 16264 (2010).

[12]T. Löffler, T. May, C. am Weg, A. Alcin, B. Hils, and H. G. Roskos, Appl. Phys. Lett. **90**, 091111 (2007).

[13]M. Ravaro, S. Barbieri, G. Santarelli, V. Jagtap, C. Manquest, C. Sirtori, S. P. Khanna, and E. Linfield, Opt. Express **20**, 25654 (2012).

[14]M. S. Vitiello, L. Consolino, S. Bartalini, A. Taschin, A. Tredicucci, M. Inguscio, and P. De Natale, Nat. Photonics **6**, 525 (2012).

[15]S. Barbieri, J. Alton, H. E. Beere, E. H. Linfield, S. Withington, D. A. Ritchie, A. Lassaad, G. Scalari, and J. Faist, Opt. Lett. **29**, 1632 (2004).

[16]A. Barkan, F. K. Tittel, D. M. Mittleman, R. Dengler, P. H. Siegel, G. Scalari, L. Ajili, J. Faist, H. E. Beere, E. H. Linfield, D. A. Ritchie, and A. G. Davies, Opt. Lett. **29**, 575 (2004).

[17]S. Barbieri, P. Gellie, G. Santarelli, L. Ding, W. Maineult, C. Sirtori, R. Colombelli, H. E. Beere, and D. A. Ritchie, Nat. Photonics **4**, 636 (2010).

[18]M. Ravaro, C. Manquest, C. Sirtori, S. Barbieri, G. Santarelli, K. Blary, J.-F. Lampin, S. P. Khanna, and E. H. Linfield, Opt. Lett. **36**, 3969 (2011).

[19]S. Barbieri, M. Ravaro, P. Gellie, G. Santarelli, C. Manquest, C. Sirtori, S. P. Khanna, H. Linfield, and A. G. Davies, Nat. Photonics **5**, 306 (2011).

[20]M. Ravaro, P. Gellie, G. Santarelli, C. Manquest, P. Filloux, C. Sirtori, J.-F. Lampin, G. Ferrari, S. P. Khanna, H. Linfield, E. H. Beere, D. A. Ritchie, and S. Barbieri, IEEE J. Sel. Top. Quantum Electron. **19**, 8501011 (2013).

[21]Note the frequency noise presented in Ref. 13 was obtained by driving the QCL with a lead-acid battery. Here the noise is significantly higher owing to the current noise of the power supply.

[22]From Ref. 13 we estimate a minimum bandwidth of $\sim$100 kHz for the PLL that locks the lock-in reference to the signal reference. For the most widely used DSP lock-in amplifiers the PLL bandwidth is of the order of a few tens of Hz. In addition, for our lock-in the reference frequency range is up to 100 kHz, which is well below the typical drift of f_{beat}, of several MHz/s.